Electronic Supplementary Material (ESI) for New Journal of Chemistry.

Metal–free C_5N_2 doped with boron atom as an efficient electrocatalyst for nitrogen reduction reaction

Tingting Zhao,[a] Yu Tian,[b] Likai Yan*[a] and Zhongmin Su [a]

[a] Institute of Functional Materials Chemistry, Key Laboratory of Polyoxometalate Science of Ministry of Education, Faculty of Chemistry, Northeast Normal University, Changchun, 130024, China

[b] Institute for Interdisciplinary Quantum Information Technology, Jilin Engineering Normal University, Changchun, 130052, China.

*To whom correspondence should be addressed.
E–mail:yanlk924@nenu.edu.cn(L. –K. Yan).

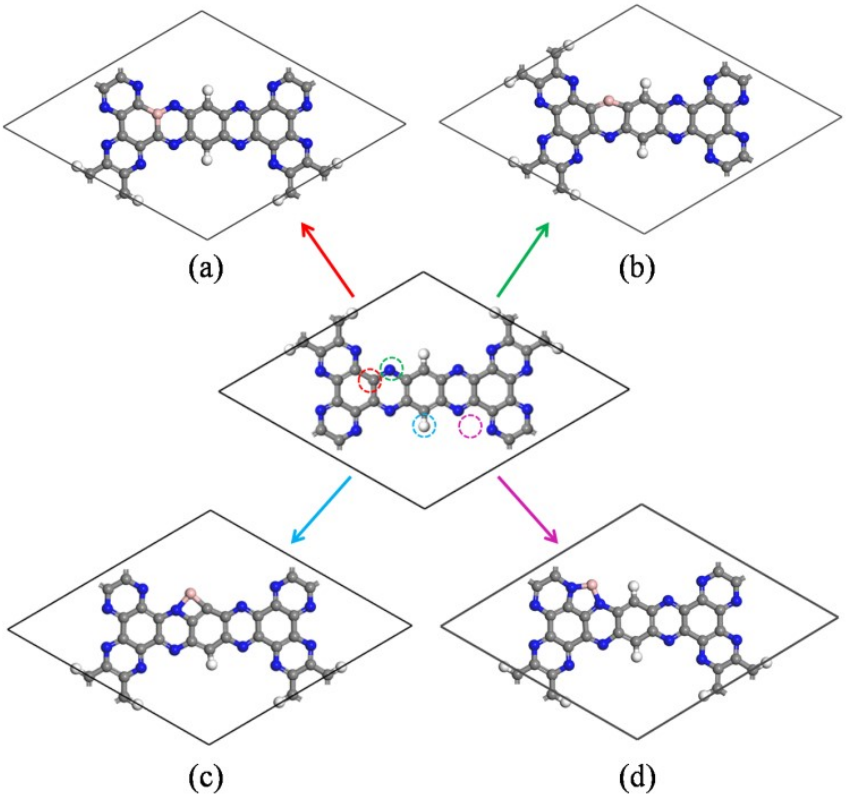

Fig. S1 The optimized structures of (a) B_C, (b) B_N, (c) B_H, and (d) B_{int}–doped C_5N_2.

Table S1 Computed free energy changes of $*NHNH_2 \rightarrow *NH_2NH_2$ on B_{int}–doped C_5N_2 using different supercell sizes.

Reaction	1 × 1	2 × 1
$*NHNH_2 \rightarrow *NH_2NH_2$	0.54	0.42

Table S2 The computed cohesive energies (E_c, eV), formation energies (E_f, eV), and the shortest distance between B and its nearest N or C atom ($d_{B\text{-}N/C}$, Å).

	B_C-C_5N_2	B_N-C_5N_2	B_H-C_5N_2	B_{int}-C_5N_2
E_c	-6.27	-6.30	-6.31	-6.30
E_f	-0.20	0.98	3.37	-0.23
$d_{B\text{-}N/C}$	1.40	1.43	1.55	1.46

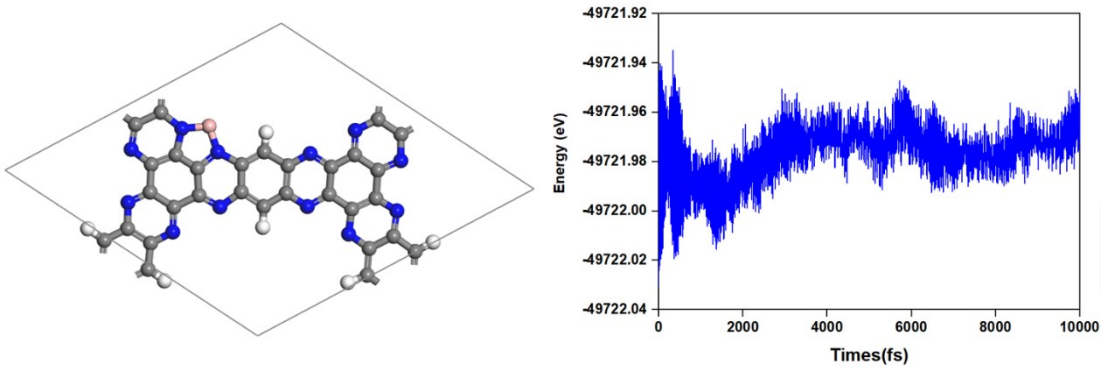

(a) (b)

Fig. S2 Geometry snapshot (a) and variations of energy (b) against time for MD simulations of B_{int}−doped C_5N_2, and the simulation is run at 500 K for 10 ps with a time step of 1 fs.

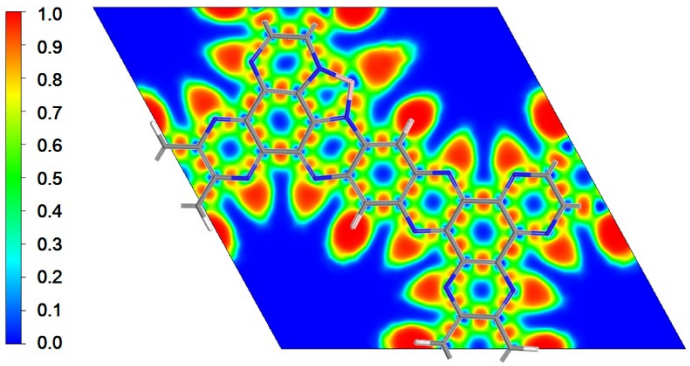

Fig. S3 Electron localization function (ELF) map of the B_{int}−doped C_5N_2. The blue and pink spheres represent N and B_{int} atoms, respectively.

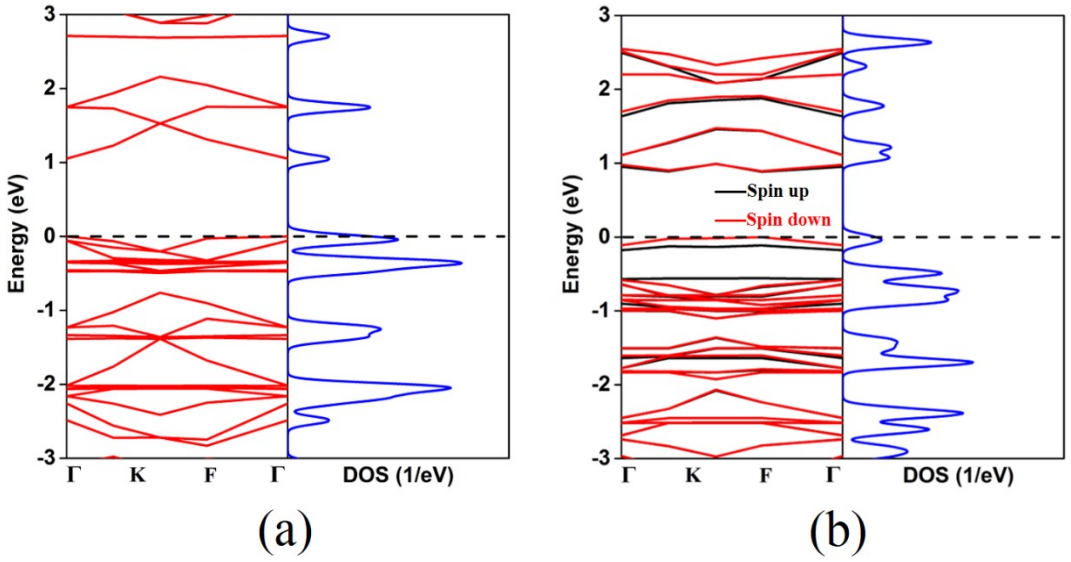

Fig. S4 Band structures and DOS for (a) C_5N_2, and (b) B_{int}–doped C_5N_2. The black and red lines in Fig. S4b represent the band structure of the spin up and spin down states, respectively.

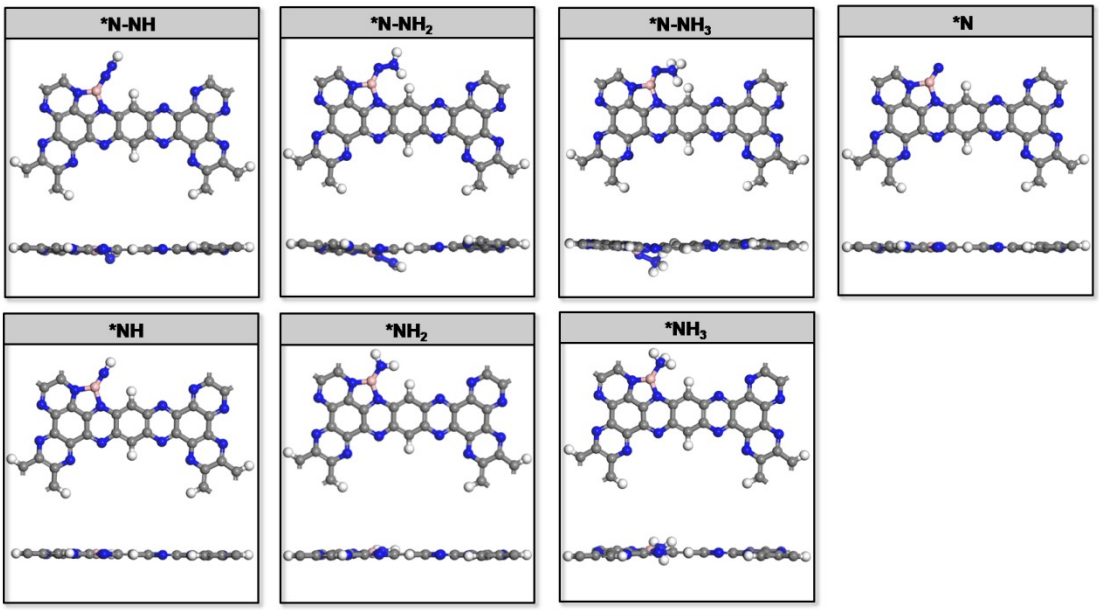

Fig. S5 Optimized structures of various reduction intermediates on B_{int}–doped C_5N_2 through the distal pathway.

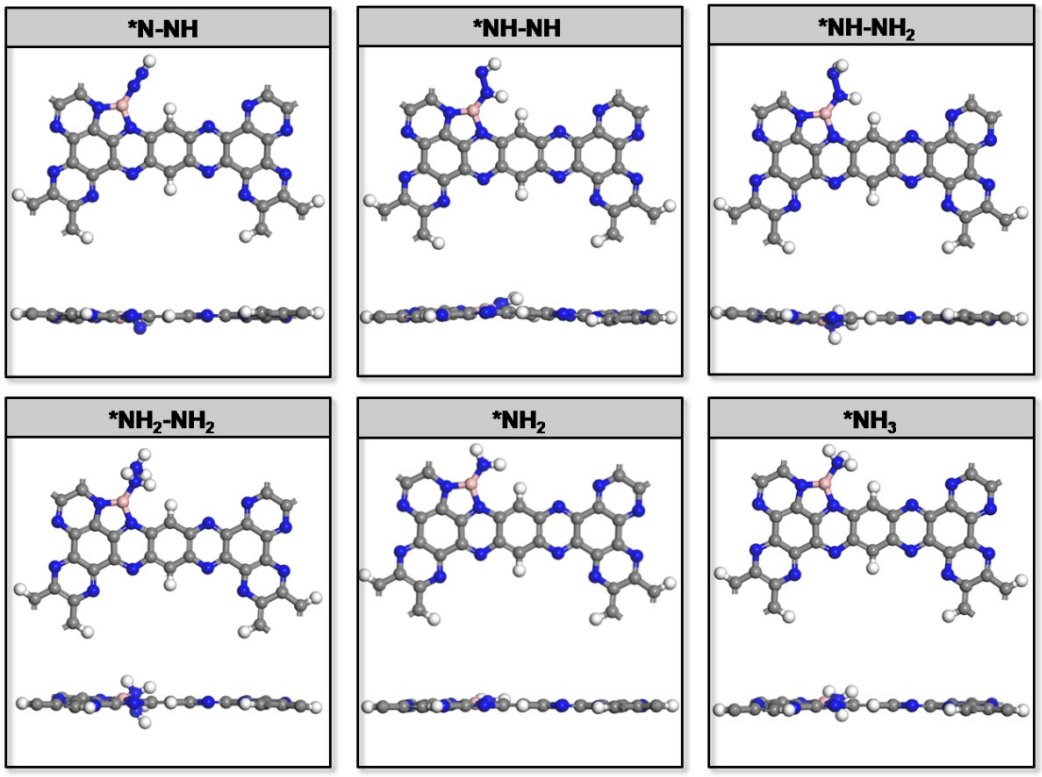

Fig. S6 Optimized structures of various reduction intermediates on B_{int}–doped C_5N_2 through the alternating pathway.

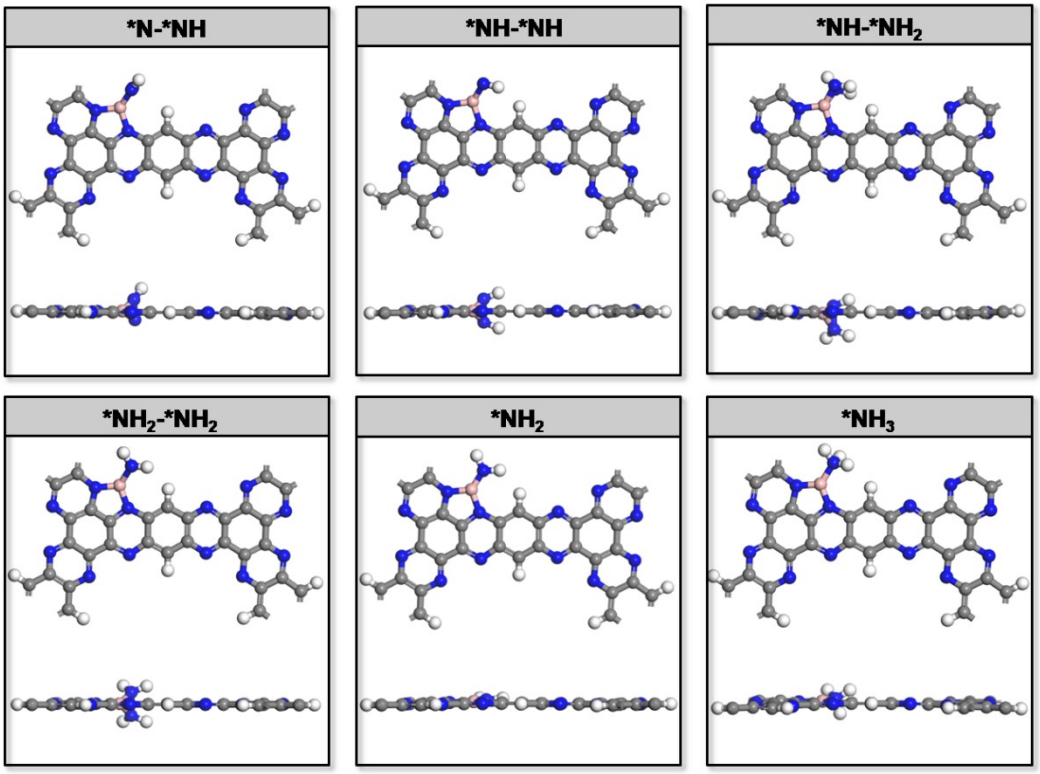

Fig. S7 Optimized structures of various reduction intermediates on B_{int}–doped C_5N_2 through the enzymatic pathway.

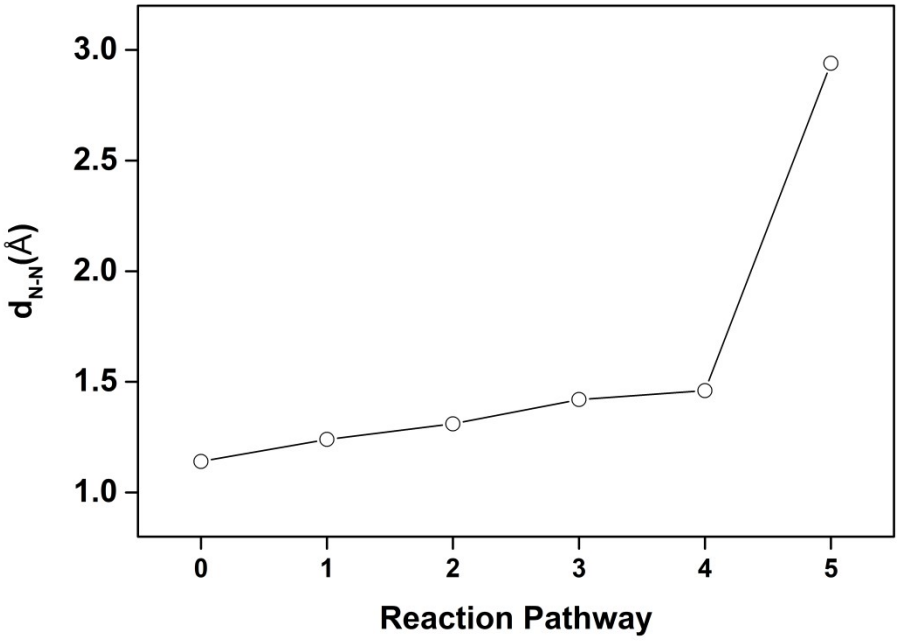

Fig. S8 The variation of the N–N bond length (d_{N-N}) along the alternating pathway *via* end-on pathway on B_{int}–doped C_5N_2. 0, 1, 2, 3, 4, and 5 represent the *N_2, *N_2H, *NH-NH, *NH-NH_2, *NH_2-NH_2, and (*NH_2 + NH_3).

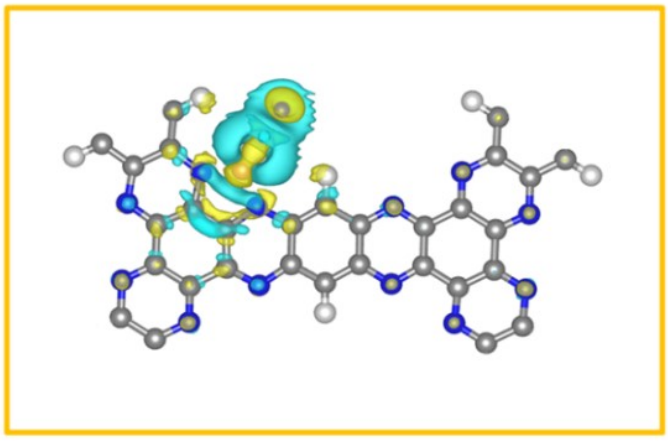

Fig. S9 The charge difference density of N_2 end–on adsorbed on the B_{int}–doped C_5N_2.

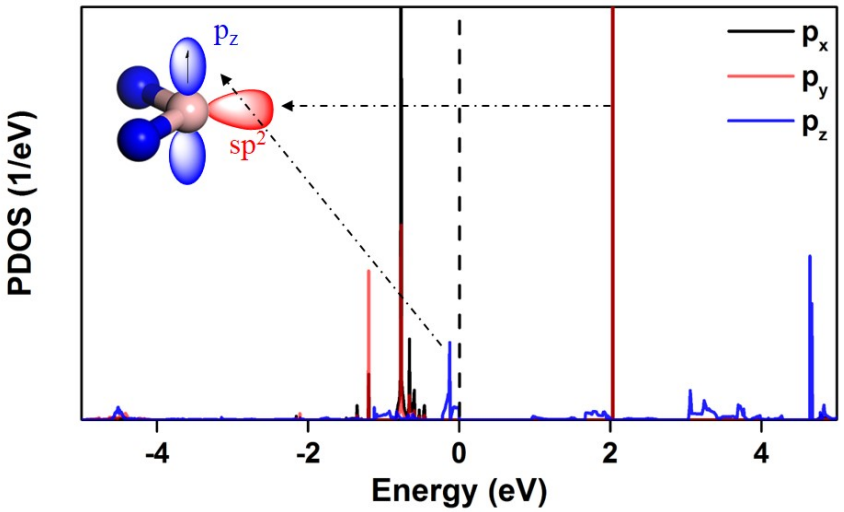

Fig. S10 The PDOS of B atoms in B_{int}–doped C_5N_2. The Fermi level is set to zero as shown by the black dotted line.

Table S3 The free energy changes of $*N_2 \rightarrow *N_2H$, $*NHNH_2 \rightarrow *NH_2NH_2$, $*NH_2 \rightarrow *NH_3$ on B_{int}–doped C_5N_2 after adding a water molecule.

Reaction	ΔG
$*N_2 \rightarrow *N_2H$	0.22
$*NHNH_2 \rightarrow *NH_2NH_2$	0.13
$*NH_2 \rightarrow *NH_3$	0.31

Table S4 Computed free energy changes of $*N_2 \rightarrow *N_2H$, $*NHNH_2 \rightarrow *NH_2NH_2$, $*NH_2 \rightarrow *NH_3$ on B, B_2, B_3, and B_4–doped C_5N_2.

Reaction	B	B_2	B_3	B_4
$*N_2 \rightarrow *N_2H$	0.40	–0.08	0.19	0.18
$*NHNH_2 \rightarrow *NH_2NH_2$	0.54	0.32	0.68	0.91
$*NH_2 \rightarrow *NH_3$	0.52	0.57	0.86	0.99